The Astrophysical Journal, 721:1158–1163, 2010 October 1 doi:10.1088/0004-637X/721/2/1158

QUANTUM LANGEVIN MOLECULAR DYNAMIC DETERMINATION OF THE SOLAR-INTERIOR EQUATION OF STATE

Jiayu Dai, Yong Hou, and Jianmin Yuan
Department of Physics, College of Science, National University of Defense Technology, Changsha 410073, China; jmyuan@nudt.edu.cn
Received 2010 July 26; accepted 2010 August 3; published 2010 September 8

ABSTRACT

The equation of state (EOS) of the solar interior is accurately and smoothly determined from ab initio simulations named quantum Langevin molecular dynamics in the pressure range of 58 Mbar $\leqslant P \leqslant 4.6 \times 10^5$ Mbar at the temperature range of 1 eV $\leqslant T \leqslant$ 1500 eV. The central pressure is calculated and compared with other models. The effect of heavy elements such as carbon and oxygen on the EOS is also discussed.

Key words: dense matter – equation of state – plasmas – Sun: interior

Online-only material: color figures

1. INTRODUCTION

For solar and stellar models, a high-quality equation of state (EOS) is very crucial (Basu & Antia 2008). It is well known that some requirements should be satisfied for solar and stellar modeling: thermodynamic quantities would be smooth, consistent, valid over a large range of temperature and density, and would incorporate the most important astrophysically relevant chemical elements (Däppen 2006) as well. Two previous major attempts to create a high-precision and high-accuracy EOS have been made, and have been included in recent opacity recalculations. They are the international Opacity Project (OP; Seatom 1995; Berrington 1997) and the Opacity Project at Livermore (OPAL). In OP, the Mihalas–Hummer–Däppen model (MHD) (Hummer & Mihalas 1988; Mihalas et al. 1988; Däppen et al. 1988; Nayfonov et al. 1999; Trampedach et al. 2006) for the EOS was developed; this model deals with *heuristic* concepts about the modification of atoms and ions in a plasma. In OPAL, the EOS relies on a *physical picture*, which is built on the modeling of electrons and nuclei. This model is called activity expansion (ACTEX) EOS (Rogers 1986; Rogers et al. 1996; Rogers & Nayfonov 2002; Iglesias & Rogers 1991). Both MHD and OPAL are dependent on the potentials between particles (electron–electron, ion–electron, and ion–ion). In addition, there are other models such as that proposed by Eggleton et al. (1973, EFF), which is thermodynamically consistent and qualitatively correct. EFF does not consider excited states, H molecule formation, or Coulomb corrections and treats full ionization for heavy elements at high density. It is interesting to note that the effect of partially degenerate electrons can be included partly according to the Fermi–Dirac statistics. In most cases, the EOS from OP, OPAL, and even EFF should be sufficient for the input parameters of stellar models. However, there are always some physics such as the coupling of ions which can be missed in these models. With increasing requirements for high precision in helioseismic study, a parameter-free model beyond the Debye–Hückel approximation for a more accurate EOS than that of OPAL and MHD is still necessary (Däppen 2006; Däppen & Nayfonov 2000).

Conditions in the solar interior are very complicated, where densities are from 10 g cm^{-3} up to 160 g cm^{-3} and temperatures are from 50 eV to 1400 eV (Bahcall et al. 2001). Hydrogen and helium are the main elements of the solar interior, making up about 98%, with small abundances of other heavy elements such as carbon, oxygen, and iron comprising the other 2%. In order to obtain an accurate and smooth EOS for the entire Sun, it is necessary to develop a model that can cover all conditions in the Sun. It is very clear that the matter in the Sun is not always ideal ionized gas plasma but moderately coupled, partly degenerate, and partly ionized (especially for heavy elements) in some area according to the definition of coupling parameter Γ and degenerate parameter θ (Ichimaru 1982), where $\Gamma = Z^{*2}/(k_{\rm B}Ta)$, with T as the system temperature, $k_{\rm B}$ as the Boltzmann constant, a signifying the mean ionic sphere radius defined as $a = (3/(4\pi n_i))^{1/3}$, Z^* representing the average ionization degree, n_i as the ionic number density, and $\theta = T/T_{\rm F}$, with the Fermi temperature $T_{\rm F} = (3\pi^2 n_e)^{2/3}/2$ (n_e is the number density of electrons). Generally speaking, when the degenerate parameter $\theta \sim 1$ and the coupled parameter $\Gamma \sim 1$, matter is considered to be partially degenerate and moderately coupled. Otherwise, if $\theta \ll 1$ ($\theta \gg 1$) and $\Gamma \gg 1$ ($\Gamma \ll 1$), matter is strongly (weakly) degenerate and strongly (weakly) coupled. For most of the regimes in the solar interior, matter is weakly coupled and weakly degenerate. However, extremely high density cannot promise negligibility of the coupling of ions, and a theory of ideal ionized gas plasma is not always appropriate. For weakly coupled or weakly degenerate matter, single atomic models such as the average atom (AA) model (Hou et al. 2006; Yuan 2002), and the detailed level accounting (DLA) model (Zeng & Yuan 2004) are assumed to be valid. Generally, the AA model is built for dense plasma, and the DLA model is used for relatively low density. Very recently, the AA model was successfully applied to astrophysical plasma (Faussurier et al. 2010). However, there is no direct physical evidence supporting these approaches, and we do not even know whether they are correct in such dense matter, or how they behave for extreme dense matter under conditions such as those found in the solar center. Therefore, it is extremely important to develop a more reliable model for all of these conditions.

For the strongly (moderately) coupled matter with partly degenerate electrons, quantum molecular dynamics (QMD), which does not require any assumptions about the potential between atoms, supplies a powerful and accurate tool and has been successfully applied to warm dense matter (WDM; Collins et al. 1995; Desjarlais et al. 2002; Mazevet et al. 2005, Mazevet & Zérah 2008). In astrophysics, QMD has been used to study the properties of giant planets and has given rise to amazingly satisfying results (Lorenzen et al. 2009; Militzer & Hubbard 2009;

Gillan et al. 2006; Vorberger et al. 2007; Nettelmann et al. 2008; Wilson & Militzer 2010). Very recently, QMD was extended to the field of high-energy density physics (HEDP) by considering the electron–ion collision induced friction (EI-CIF) in molecular dynamics, and a corresponding model called quantum Langevin molecular dynamics (QLMD) was constructed (Dai & Yuan 2009; Dai et al. 2010). Thanks to this model, one can study the properties of matter in the regime of HEDP from first principles. It is also a good tool for investigating a system in which the coupling of ions is important.

In this work, we first study the EOS of conditions in the solar interior using QLMD. Three densities with different temperatures are chosen, and their EOSs are compared with the EOS of the AA model with energy-level broadening (AAB; Hou et al. 2006). QLMD can ensure much more accurate results in all conditions and agrees with AAB at high temperatures. The central pressure of the Sun is also calculated using the QLMD and AA models, which are compared with the data from OP, OPAL, EFF, and standard solar models (Bahcall et al. 2001). The important effect of heavy elements on the EOS of very dense matter is also investigated.

2. THEORETICAL METHOD

2.1. Quantum Langevin Molecular Dynamics

First we recall the QLMD method, where electronic structure is studied from density functional theory (DFT) and ionic trajectory is performed using the Langevin equation (Dai et al. 2010)

$$M_I\ddot{\mathbf{R}}_\mathbf{I} = \mathbf{F} - \gamma M_I\dot{\mathbf{R}}_\mathbf{I} + \mathbf{N}_\mathbf{I}, \tag{1}$$

where M_I is the ionic mass, $\mathbf{F}$ is the force calculated in DFT, γ is a Langevin friction coefficient, $\mathbf{R}_\mathbf{I}$ is the position of ions, and $\mathbf{N}_\mathbf{I}$ is a Gaussian random noise corresponding to γ. Considering the dynamical collisions between electrons and ions at high temperature, the friction coefficient γ can be estimated by

$$\gamma = 2\pi\frac{m_e}{M_I}Z^*\left(\frac{4\pi n_i}{3}\right)^{1/3}\sqrt{\frac{k_\mathrm{B}T}{m_e}}, \tag{2}$$

where m_e is the electronic mass and Z^*, n_i, and T are defined in the previous section. Therefore, the dynamical electron–ion collisions at high temperature can be described as a friction or noise effect. By introducing this dynamical EI-CIF, the first principles simulations can be applied in the HEDP regime, overcoming the difficulty of numerical calculations, and therefore give more reliable results.

To guarantee an accurate sampling of the Maxwell–Boltzmann distribution, the noise has to obey the fluctuation-dissipation theorem:

$$\langle\mathbf{N}_\mathbf{I}(0)\mathbf{N}_\mathbf{I}(t)\rangle = 6\gamma M_I k_\mathrm{B}T\,dt, \tag{3}$$

where dt is the time step of molecular dynamics. At the same time, the random forces are taken from a Gaussian distribution of mean zero and variance of $\langle\mathbf{N}_\mathbf{I}{}^2\rangle = 6\gamma M_I k_\mathrm{B}T/dt$.

In order to integrate Equation (1), the formalism in a Verlet-like form (Pastor et al. 1988) integration is performed as follows:

$$\mathbf{R}_\mathbf{I}(t+dt) = \mathbf{R}_\mathbf{I}(t) + (\mathbf{R}_\mathbf{I}(t) - \mathbf{R}_\mathbf{I}(t-dt))\frac{1-\frac{1}{2}\gamma_T dt}{1+\frac{1}{2}\gamma_T dt} + (dt^2/M_I)(\mathbf{F}_\mathbf{BO}(t) + \mathbf{N}_\mathbf{I}(t))\left(1+\frac{1}{2}\gamma_T dt\right)^{-1}. \tag{4}$$

The velocities of ions $\mathbf{v}_\mathbf{I}(t+dt)$ can also be calculated by using the Verlet formula

$$\mathbf{v}_\mathbf{I}(t+dt) = \dot{\mathbf{R}}_\mathbf{I} = \frac{\mathbf{R}_\mathbf{I}(t+dt) - \mathbf{R}_\mathbf{I}(t-dt)}{2dt}. \tag{5}$$

This ab initio molecular dynamic model based on the Langevin equation is named QLMD, which extends the applications of an ab initio method into the field of HEDP. Based on QLMD, the effects of coupled ions and degenerate electrons can be studied, which can yield much more accurate results at relatively low temperature and high density. It is worth pointing out that the computational cost of QLMD is very expensive under conditions of very weakly coupled and non-degenerate matter. In such a case the existing models such as MHD, ACTEX, and the AA model can provide consistent and accurate data.

2.2. Average Atom Model with Electronic Energy-level Broadening

The AA model is one of the statistical approximations applied to study the electronic structure of atoms and ions in hot dense plasmas, which can easily be applied in conjunction with a variety of treatments of electron orbitals in atoms. In a full relativistic self-consistent field-based AA model, the influence of the environment on the atom is assumed to be spherically symmetric on average. The movement of an electron during interactions of the nucleus and other electrons is approximated by a central field, which is determined by the standard self-consistent calculation. In the central field, the radial part of the Dirac equation has the form:

$$\begin{cases}\dfrac{dP_{n\kappa}(r)}{dr} + \dfrac{\kappa}{r}P_{n\kappa}(r) = \dfrac{1}{c}[\epsilon + c^2 - V(r)]Q_{n\kappa}(r)\\ \dfrac{dQ_{n\kappa}(r)}{dr} - \dfrac{\kappa}{r}Q_{n\kappa}(r) = -\dfrac{1}{c}[\epsilon - c^2 - V(r)]P_{n\kappa}(r)\end{cases}, \tag{6}$$

where $P(r)$ and $Q(r)$ are, respectively, the large and small components of the wave function, c is the speed of light, and $V(r)$ is the self-consistent potential, consisting of three parts, which are, respectively, the static, exchange, and correlation potentials. The static part is calculated from the charge distributions in the atom, while the exchange and correlation parts take the approximate forms described by Dharma-Wardana & Taylor (1981). For bound states, the boundary conditions are satisfied by the radial wave functions

$$\begin{cases}P_{n\kappa}(r) \xrightarrow{r\to 0} ar^{l+1}\\ P_{n\kappa}(R_b) = 0\end{cases} \text{ or } \begin{cases}P_{n\kappa}(r) \xrightarrow{r\to 0} ar^{l+1}\\ \dfrac{d}{dr}\left[\dfrac{P_{n\kappa}(r)}{r}\right]_{R_b} = 0\end{cases}, \tag{7}$$

where R_b is the radius of the atom. The electron distribution is calculated separately for the bound and free electron parts. The bound electron density is obtained according to

$$D_b(r) = \frac{1}{4\pi r^2}\sum_j b_j\left(P_j^2(r) + Q_j^2(r)\right), \tag{8}$$

where b_j is the occupation number of the state j. In the AA model without energy-level broadening (AANB), the occupation number b_j is determined by the Fermi–Dirac distribution

$$b_j = \frac{2|\kappa_j|}{\exp((\epsilon_j - \mu)/T) + 1}. \tag{9}$$

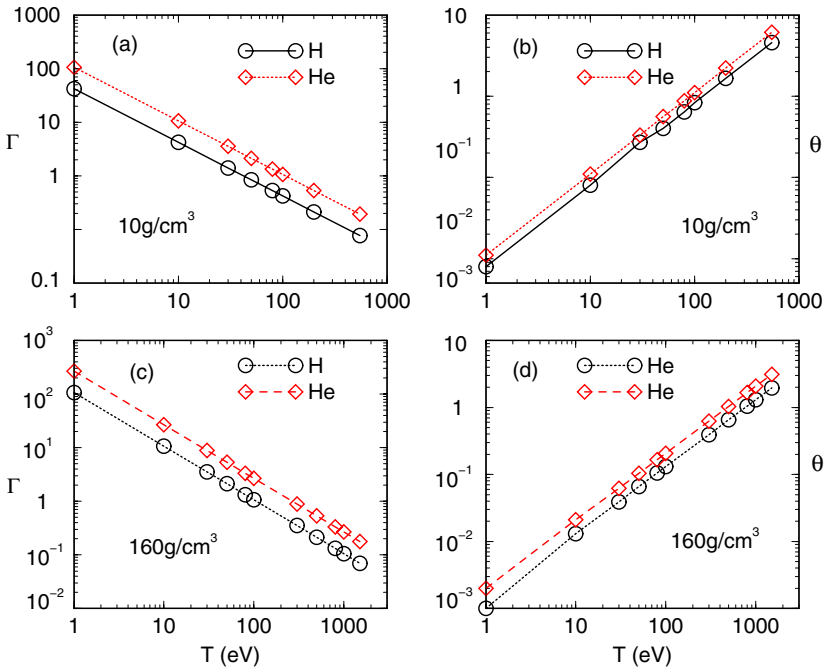

Figure 1. Coupling parameters (Γ) and degenerate parameters (θ) of H and He from 1 eV to 550 eV at a density of 10 g cm^{-3} ((a) and (b)), and from 1 eV to 1500 eV at a density of 160 g cm^{-3} ((c) and (d)).

(A color version of this figure is available in the online journal.)

In order to consider the effect of energy-level broadening, Gaussian functions $\rho(\epsilon)$ centered at the corresponding electron orbital energies of Equation (7) are introduced into the Fermi–Dirac distribution of electrons, i.e.,

$$b_j(\epsilon) = \frac{2|\kappa_j|\rho(\epsilon)}{\exp((\epsilon_j - \mu)/T) + 1} \tag{10}$$

and

$$D_b(r) = \frac{1}{4\pi r^2} \sum_j \int_a^b b_j(\epsilon)\left(P_j^2(r) + Q_j^2(r)\right)d\epsilon, \tag{11}$$

where $1 = \int_a^b \rho(\epsilon)d\epsilon$ and the two orbital energies obtained from the boundary conditions of Equation (7) are taken as the upper and lower half maximum positions of the Gaussian form energy-level broadening.

Based on this approach, the splitting of the real energy levels approximated by the energy-level broadening can be considered, which makes the irregularities caused by the pressure-induced electron ionization without energy-level broadening disappear naturally (Hou et al. 2006, 2007).

3. RESULTS AND DISCUSSIONS

3.1. Computational Details

For the study of the solar-interior EOS, we choose three typical densities in the solar interior: 10 g cm^{-3} (radiative zone), 100 g cm^{-3}, and 160 g cm^{-3} (core). Temperatures from 1 eV to 550 eV for 10 g cm^{-3} and from 10 eV to 1500 eV for 100 and 160 g cm^{-3} are calculated, covering the conditions from the radiative zone into the core. Since the H and He elements make up about 98% of the composition of the Sun (Lodders 2003), we calculated four structures with different compositions (using X to represent the mass abundance of H, Y for the abundance of He, and Z for the abundances of other elements), which are $X = 1$, $Y = 0$, $Z = 0$; $X = 0$, $Y = 1$, $Z = 0$; $X = 0.7$, $Y = 0.3$, $Z = 0$; and $X = 0.40$, $Y = 0.60$, $Z = 0$. Supercells containing $T = 125$ particles for 10 g cm^{-3} and $T = 256$ particles for 100 g cm^{-3} and 160 g cm^{-3} are constructed. When $Z = 0$, the number of H atoms ($N_{\rm H}$) and He atoms ($N_{\rm He}$) can be calculated by the formulae:

$$\frac{4N_{\rm He}}{4N_{\rm He} + N_{\rm H}} = Y, \quad N_{\rm He} + N_{\rm H} = T. \tag{12}$$

In these conditions, the matter changes from strongly coupled to relatively weakly coupled and from partially degenerate to weakly degenerate, as shown in Figure 1, where QLMD has been successfully proved.

For the QLMD simulations, we have used the Quantum Espresso package (Giannozzi et al. 2009) based on the finite temperature DFT. The Perdew–Zunger parameterization of local density approximation (LDA; Perdew & Zunger 1981) is used for the exchange-correlation potential. Similar to the calculation of hydrogen at a density of 80 g cm^{-3} (Dai et al. 2010; Recoules et al. 2009), the Coulombic pseudopotentials with a cutoff radius of 0.005 a.u. for H and He are adopted. The plane wave cutoff energy is between 200 Ry and 400 Ry with an increase in temperature. As discussed in Recoules et al. (2009), pressure delocalization promises that the upper band electronic eigenstates are nearly plane waves, and thus the basis set is greatly reduced. Therefore, even though we choose a large number of bands in order to ensure the accuracy of the calculation, the computational cost is not very expensive. In our cases, we used enough bands in order to make the corresponding band energies higher than $8k_{\rm B}T$ (especially at high temperature). The gamma point only is used for the representation of the Brillouin zone. We tested all of these parameters carefully, and found that adding more k-points, more bands, a larger energy cutoff, or more particles does not

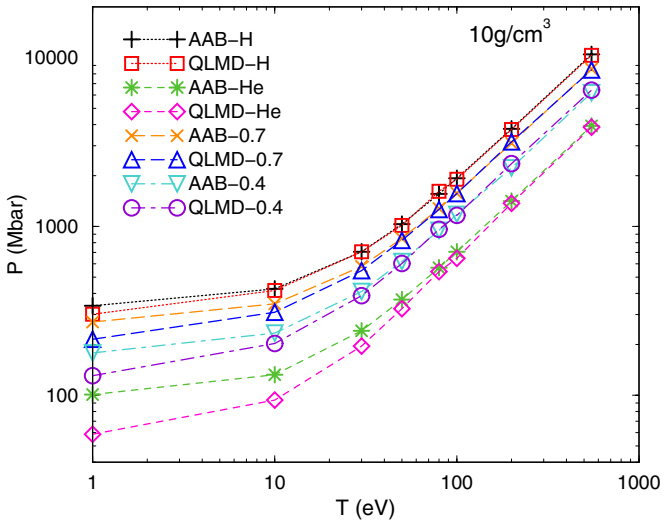

Figure 2. Pressure vs. temperature for a density of 10 g cm^{-3} with different chemical compositions compared with the results of AAB. In the figure, 0.7 represents $X = 0.7$ and 0.4 represents $X = 0.4$.

(A color version of this figure is available in the online journal.)

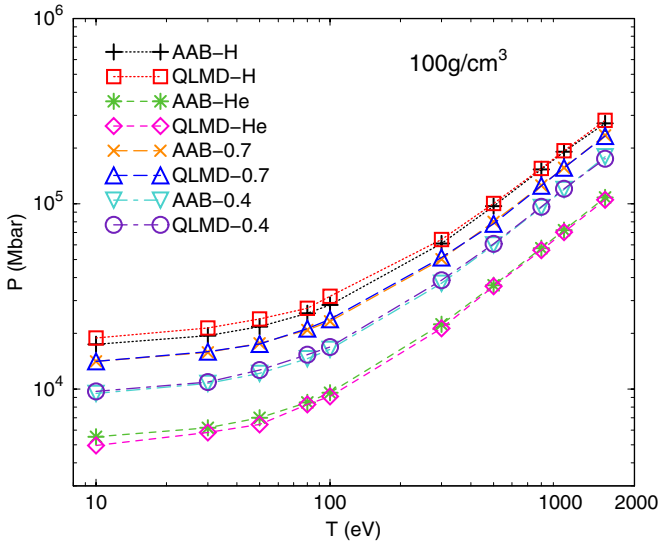

Figure 3. Pressure vs. temperature for a density of 100 g cm^{-3} with different chemical compositions compared with the results of AAB.

(A color version of this figure is available in the online journal.)

result in any significant difference. The time step of QLMD is $a_I/(20\sqrt{k_B T M_I})$ (Recoules et al. 2009), where a_I and M_I are the average ionic radius and the ionic mass of the Ith ion, respectively. After thermalization, each structure is simulated for 5000–10,000 time steps to pick up the useful information.

3.2. Equation of State

First, we study the isochoric heating curve along a density of 10 g cm^{-3} from 1 eV to 550 eV under the conditions of the solar radiative zone. Comparisons between the pressures calculated using the QLMD and AAB models for different compositions are given in Figure 2. It is shown that for the system of He with two electrons at lower temperatures, the pressure of the AAB model is much larger than that of the QLMD model. However, the relative difference for H is not as big as for He. Therefore, with an increase in both temperature and the abundance of hydrogen, the gap between the QLMD and AAB models becomes smaller. It is very clear that more electrons and low temperature result in difficulties in describing the ionization balance for the AAB model, where the composition of the system is complicated. Strong coupling among the ions, which is included in the QLMD model but not in the AAB model, also plays an important role also in the calculations. Here, we recall that the simple way to calculate the EOS containing only one element and averaging the pressure according to the mass ratio is not accurate enough, as discussed in Yuan (2002). For example, for the density–temperature point (10 g cm^{-3} and 10 eV) and composition ($X = 0.7$, $Y = 0.3$, and $Z = 0$), the average pressure is $P_a = (0.7 \times 301.3 + 0.3 \times 58.6) = 228.49$ Mbar. However, the pressure of this mixture obtained using QLMD is 214.77 Mbar, and the error is about 6%, which is significant for astrophysical applications.

In conditions deeper in the solar interior, some interesting characteristics appear. For a density of 100 g cm^{-3}, the pressure–temperature relation is shown in Figure 3. Moreover, the maximum density of the Sun is about 160 g cm^{-3}, whose isochoric heating curve from 10 eV to 1500 eV is shown in Figure 4. Contrary to the relative difference between the QLMD and AAB models in Figure 2, the pressures of the AAB model for 100 and 160 g cm^{-3} are smaller than those of the QLMD

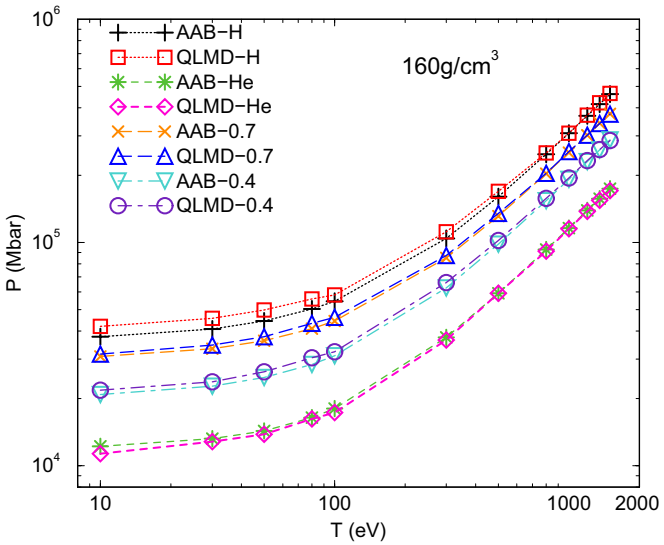

Figure 4. Pressure vs. temperature for a density of 160 g cm^{-3} with different chemical compositions compared with the results of AAB.

(A color version of this figure is available in the online journal.)

model, especially for one component, H. In fact, a spherical assumption (Yuan 2002) for ions in the AAB model makes the effective volume of the system larger than the real one, giving rise to smaller pressure. This phenomenon is obvious when the density is high enough, such as 160 g cm^{-3} for H here. With the increase in temperature, the pressure of AAB and QLMD becomes consistent. At high temperatures, the ions are weakly coupled and electrons are almost free. Therefore, semiclassical methods such as the Thomas–Fermi method and AAB can work well. Furthermore, it can be deduced that the EOS of the entire area of the Sun can be obtained accurately and smoothly, which is beyond the OP and OPAL models, and completely parameter-free.

For the central conditions in the Sun, the density reaches up to 152.7 g cm^{-3} and the temperature reaches up to 15,696,000 K according to the standard solar model (Bahcall et al. 2001). The central pressure is also about 2.342×10^5 Mbar, which

Table 1
Comparison of Central Pressures of the Sun at Typical Temperature (T) and Density (ρ)

ρ (g cm^{-3})	T (eV)	EOS Model	Pressure (Mbar)
141.25	989.45	EFF	1.6396×10^5
		LIV	1.6162×10^5
		MHD	1.6190×10^5
		AANB	1.6144×10^5
		AAB	1.5922×10^5
		QLMD	1.6090×10^5
141.25	1189.58	EFF	1.9579×10^5
		LIV	1.9337×10^5
		MHD	1.9365×10^5
		AANB	1.9330×10^5
		AAB	1.9027×10^5
		QLMD	1.9122×10^5
152.70	1352.64	Standard	2.3420×10^5
		AANB[a]	2.3603×10^5
		AAB[a]	2.3417×10^5
		QLMD[a]	2.3525×10^5
		AANB[b]	2.2678×10^5
		AAB[b]	2.2534×10^5
		QLMD[b]	2.2575×10^5
		AANB[c]	2.2445×10^5
		AAB[c]	2.2301×10^5
		QLMD[c]	2.2328×10^5

Notes. Results of EFF, LIV (OPAL), and MHD from Däppen et al. (1990; $X = 0.34828$, $Y = 0.65172$, and $Z = 0$). Results of AANB, AAB, and the standard solar model (Standard; Bahcall et al. 2001) are also compared. Pressures of the chemical composition of H, He, and C with $X = 0.3387$, $Y = 0.6613$, and $Z = 0$ ([a]), $X = 0.3125$, $Y = 0.6406$, and $Z = 0.0469$ ([b]), and the chemical composition of H, He, and O with $X = 0.3077$, $Y = 0.6308$, and $Z = 0.0615$ ([c]) are also shown.

has previously never been reached from the first principles simulation. Based on QLMD, we solved this problem from an ab initio approach and obtained the EOS under this condition. We first compared the pressure close to the solar center with other models, as shown in Table 1, and they agree reasonably well with each other. It is interesting to find that the pressure of AANB is much larger than those found with QLMD and AAB, and consistent with the EFF, Livermore (LIV), and MHD (Däppen et al. 1990) models. Since QLMD can be realized much more reliably, we can think that AAB is more reasonable, and both QLMD and AAB can improve the accuracy of the EOS much. In fact, for the very dense medium, the electronic structures of elements are not only the energy levels, but also the energy bands. It is reasonable to consider the effect of energy-level broadening, which is naturally included in QLMD and thus gives rise to appropriate results. For the solar central regime, we calculate the pressure with different compositions. First of all, we consider the chemical compositions of H and He, with abundances $X = 0.34828$, $Y = 0.65172$, and $Z = 0.0$. It is found that the pressures of QLMD and AAB are almost equal within 0.5% error and are very similar to the standard. The small difference between them is caused by a lack of heavier elements. In order to understand the effect of heavier elements on the EOS, we study the pressure of chemical compositions of H, He, and C and H, He, and O, respectively. As shown in Table 1, the existence of heavier elements decreases the pressure a little since the abundance is very small. In principle, we can calculate the conditions of the solar interior with any composition and any abundance using QLMD which results in an accurate and smooth EOS, particularly at relatively low temperatures and high densities. QLMD can also be very complementary to the AA models considering the computational cost, and significantly improve the accuracy of the EOS in the solar interior.

In conclusion, the EOS of the solar interior is calculated based on the first principles method of QLMD, which is more complex and reliable than the MHD and OPAL models. Furthermore, the QLMD model can promise accuracy for the EOS and be complementary to AA-like models. Accuracy can be improved significantly, particularly at relatively low temperatures and high densities where the coupling of ions cannot be neglected. It provides us with a useful tool for investigating the properties of the Sun and Sun-like stars from ab initio approaches, which is very powerful in astrophysics. This work can also open a new field of investigating solar or stellar properties from first principles, showing the importance of ionic coupling for theory and giving us more accurate data for experiment.

This work is supported by the National Natural Science Foundation of China under grant Nos. 10734140, 60921062, and 10676039, and the National Basic Research Program of China (973 Program) under grant No. 2007CB815105. Calculations were carried out at the Research Center of Supercomputing Application, NUDT. The authors thank the anonymous reviewer.

REFERENCES

Bahcall, J. N., Pinsonneault, M. H., & Basu, S. 2001, ApJ, 555, 990
Basu, S., & Antia, H. M. 2008, Phys. Rep., 457, 217
Berrington, K. A. 1997, The Opacity Project, Vol. II (Bristol: IOP publishing)
Collins, L., et al. 1995, Phys. Rev. E, 52, 6202
Dai, J., Hou, Y., & Yuan, J. 2010, Phys. Rev. Lett., 104, 245001
Dai, J., & Yuan, J. 2009, Europhys. Lett., 88, 20001
Däppen, W. 2006, J. Phys. A: Math. Gen., 39, 4441
Däppen, W., Lebreton, Y., & Rogers, F. 1990, Sol. Phys., 128, 35
Däppen, W., Mihalas, D., Hummer, D. G., & Mihalas, B. W. 1988, ApJ, 332, 261
Däppen, W., & Nayfonov, A. 2000, ApJS, 127, 287
Desjarlais, M. P., Kress, J. D., & Collins, L. A. 2002, Phys. Rev. E, 66, 025401
Dharma-Wardana, M. W. C., & Taylor, R. 1981, J. Phys. C: Solid State Phys., 14, 629
Eggleton, P., Faulkner, J., & Flannery, B. P. 1973, A&A, 23, 325
Faussurier, G., Blancard, C., Cossé, P., & Renaudin, P. 2010, Phys. Plasmas, 17, 052707
Giannozzi, P., et al. 2009, J. Phys.: Condens. Matter, 21, 395502
Gillan, M. J., Alfè, D., Brodholt, J., Vocadlo, L., & Price, G. D. 2006, Rep. Prog. Phys., 69, 2365
Hou, Y., Jin, F., & Yuan, J. 2006, Phys. Plasmas, 13, 093301
Hou, Y., Jin, F., & Yuan, J. 2007, J. Phys.: Condens. Matter, 19, 425204
Hummer, D. G., & Mihalas, D. 1988, ApJ, 331, 794
Ichimaru, S. 1982, Rev. Mod. Phys., 54, 1017
Iglesias, C. A., & Rogers, F. J. 1991, ApJ, 371, 408
Iglesias, C. A., & Rogers, F. J. 1993, ApJ, 412, 752
Iglesias, C. A., & Rogers, F. J. 1995, ApJ, 443, 460
Iglesias, C. A., & Rogers, F. J. 1996, ApJ, 464, 943
Lodders, K. 2003, ApJ, 591, 1220
Lorenzen, W., Holst, B., & Redmer, R. 2009, Phys. Rev. Lett., 102, 115701
Mazevet, S., Desjarlais, M. P., Collins, L. A., Kress, J. D., & Magee, N. H. 2005, Phys. Rev. E, 71, 016409
Mazevet, S., & Zérah, G. 2008, Phys. Rev. Lett., 101, 155001
Mihalas, D., Däppen, W., & Hummer, D. G. 1988, ApJ, 331, 815
Militzer, B., & Hubbard, W. B. 2009, Ap&SS, 322, 129
Nayfonov, A., Däppen, W., Hummer, D. G., & Mihalas, D. M. 1999, ApJ, 526, 451
Nettelmann, N., Holst, B., Nettelmann, A., French, M., & Redmer, R. 2008, ApJ, 683, 1217
Pastor, R. W., Brooks, B. R., & Szabo, A. 1988, Mol. Phys., 65, 1409
Perdew, J. P., & Zunger, A. 1981, Phys. Rev. B, 23, 5048
Recoules, V., Lambert, F., Decoster, A., Canaud, B., & Clérouin, J. 2009, Phys. Rev. Lett., 102, 075002

Rogers, F. J. 1986, ApJ, 310, 723
Rogers, F. J., & Nayfonov, A. 2002, ApJ, 576, 1064
Rogers, F. J., Swenson, F. J., & Iglesias, C. A. 1996, ApJ, 456, 902
Seaton, M. J. 1995, The Opacity Project, Vol. I (Bristol: IOP publishing)
Trampedach, R., Däppen, W., & Baturin, V. A. 2006, ApJ, 646, 560
Vorberger, J., Tamblyn, I., Militzer, B., & Bonev, S. A. 2007, Phys. Rev. B, 75, 024206
Wilson, H. F., & Militzer, B. 2010, Phys. Rev. Lett., 104, 121101
Yuan, J. 2002, Phys. Rev. E, 66, 047401
Zeng, J., & Yuan, J. 2004, Phys. Rev. E, 70, 027401